Eur. Phys. J. A **27**, 199–205 (2006)
DOI 10.1140/epja/i2005-10266-0

THE EUROPEAN PHYSICAL JOURNAL A

Partial wave analysis of $\pi^+\pi^-\pi^0$ production in two-photon collisions at LEP

V.A. Schegelsky, A.V. Sarantsev[a], A.V. Anisovich, and M.P. Levchenko

Petersburg Nuclear Physics Institute, Gatchina, Russia

Received: 25 November 2005 / Revised version: 13 February 2006 /
Published online: 31 March 2006 –
Communicated by A. Schäfer

Abstract. The reaction $\gamma\gamma \to \pi^+\pi^-\pi^0$ with quasi-real photons is studied with a total integrated luminosity of $663\,\mathrm{pb}^{-1}$, collected by the L3 detector at LEP at center-of-mass energies from 183 to 209 GeV. The results of an energy-dependent partial wave analysis in the mass region $1.1 \leq M(\pi^+\pi^-\pi^0) \leq 2.2\,\mathrm{GeV}$ are presented. The reaction is dominated by $a_2(1320)$ formation. A strong signal consistent with the first radial excitation of the isovector tensor state, $a_2(1700)$, is present and confirms the previous L3 observation. Its two-photon partial width is found to be $\Gamma_{\gamma\gamma}Br(3\pi) = 0.37^{+0.12}_{-0.08}\,\mathrm{keV}$, the relative branching ratio of $\rho(770)\pi$ to $f_2(1270)\pi$ is 3.4 ± 0.4. For all observed states the product of $\gamma\gamma$ partial width and 3π branching ratios is measured.

PACS. 11.80.Et Partial-wave analysis – 13.60.Le Meson production – 13.25.-k Hadronic decays of mesons – 14.40.-n Mesons

1 Introduction

In this report we present the analysis of the $\pi^+\pi^-\pi^0$ final state from the two-photon reaction

$$e^+e^- \to e^+e^-\pi^+\pi^-\pi^0$$

based on the data taken by the L3 experiment at LEP at center of mass energies $183 \leq \sqrt{s} \leq 209\,\mathrm{GeV}$. The data were taken during the years 1997 to 2000 with an integrated luminosity of $663\,\mathrm{pb}^{-1}$.

The process $\gamma\gamma \to \pi^+\pi^-\pi^0$ has been investigated by several experiments [1] at lower values of $\sqrt{s}$. The $\pi^+\pi^-\pi^0$ spectrum is dominated by the 2^{++} resonance $a_2(1320)$. The analysis of the L3 data [2] at $\sqrt{s} \simeq 91\,\mathrm{GeV}$, with an integrated luminosity of $140.6\,\mathrm{pb}^{-1}$, showed evidence for another 2^{++} resonance at mass of $1752 \pm 21 \pm 4\,\mathrm{MeV}$ and a width of $150 \pm 110 \pm 34$.

Two-photon interactions provide an important tool for the investigation of hadronic resonances due to their selectivity of allowed final states. The two-photon channel couples only to states, R, with positive C-parity. Since a three-pion final state has a negative G-parity and $G = Ce^{i\pi I}$ for a neutral system, only isovector states can be produced in the $\gamma\gamma \to \pi^+\pi^-\pi^0$ reaction. Due to conservation of C-parity in neutral decay modes, only $q\bar{q}$-states with $J^{PC} = 0^{++}$, 2^{++}, $4^{++}\ldots$ are produced in the $\pi^+\pi^-$ subsystem and only states with $J^{PC} = 1^{--}$, $3^{--}, \ldots$ are allowed in the $\pi^\pm\pi^0$ subsystem.

In this paper, resonances decaying to the different final states are identified by an energy-dependent partial wave analysis [3], which assumes the cascade decay, $R \to R'\pi$, and the interference between different amplitudes is taken into account. The masses and widths of resonances produced in $\gamma\gamma$ channel, defined as poles of the scattering amplitude are obtained as well as the branching ratios for decays into different $R'\pi$ channels. For all found states the two-photon partial widths, $\Gamma_{\gamma\gamma}Br(3\pi)$ were calculated from the measured amplitude. For 2^{++} resonances we also define the ratio between two-photon S- and D-wave initial states.

To determine the experimental efficiency for the $e^+e^- \to e^+e^-\pi^+\pi^-\pi^0$ reaction the EGPC [4] Monte Carlo generator is used. It describes the cross-section of the two-photon process as the product of the luminosity function for transverse photons and the cross-section of the $\pi^+\pi^-\pi^0$ production, generated according to Lorentz-invariant phase space. Events are passed through the L3 detector simulation based on the GEANT [5] and GEISHA [6] programs.

2 Event selection

The L3 detector [7] is suitable for the study of resonances produced in two-photon collisions due to its good effi-

[a] e-mail: andsar@pnpi.spb.ru

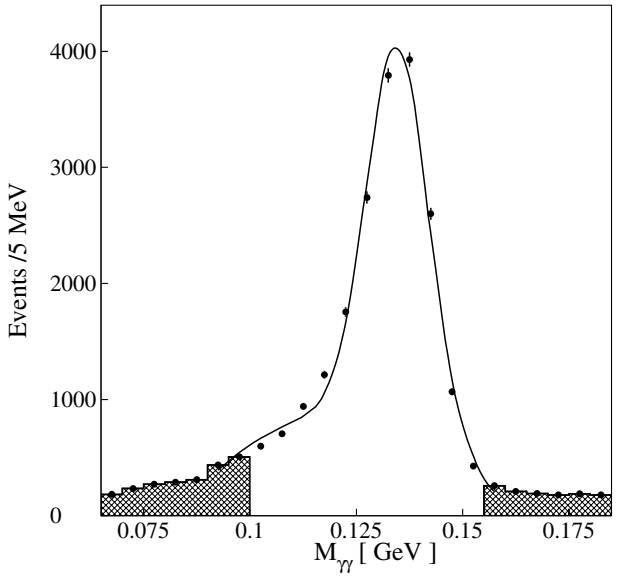

Fig. 1. Effective mass of two candidate photons. The Gaussian fit with a polynomial background shows good energy calibration (the mass of π^0 is (134.5 ± 0.6) MeV) and resolution (7 MeV). The side bands of π^0, used to evaluate the background, are indicated as shaded areas.

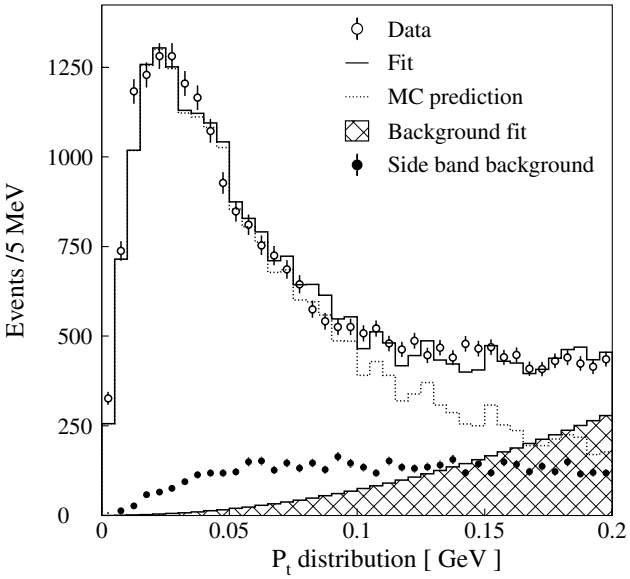

Fig. 2. Total transvers momentum distribution used to estimate the background. The background, estimated from the side bands of π^0, is also shown.

ciency and acceptance for low-energy photons and charged particles. The events are mainly accepted by the charged-particle trigger [8], which requires at least two charged particles with a transverse momentum $\mathbf{p}_t > 100$ MeV, back to back, within a complanarity angle of $\pm 41°$, and the inner track trigger [9]. This last trigger extends the polar angle acceptance from $30 < \theta < 150°$ to $15 < \theta < 165°$ and has practically no requirement on the complanarity angle of the tracks.

The $\pi^+\pi^-\pi^0$ final state is selected by requiring:

1. Two charged tracks with a net charge of zero. The tracks must come from the interaction vertex within three standard deviations.
2. Two photon candidates, reconstructed from isolated electromagnetic showers in the fiducial polar angle region of the detector $14 < \theta < 35°$, $145 < \theta < 166°$ and $45 < \theta < 135°$. A shower is isolated if the angular difference $(\Delta\theta^2 + \Delta\Phi^2)^{1/2}$ from all tracks is greater than 0.2 rad. The reconstructed electromagnetic showers have energy greater than 50 MeV.
3. One π^0 with a mass between 95 MeV and 155 MeV, formed by at least one photon candidate of energy greater than 80 MeV (fig. 1).

For a total luminosity of 663 pb^{-1}, 18000 events are selected.

There are different kinds of background in the $\pi^+\pi^-\pi^0$ sample.

– The first source of background is two charged-particle exclusive events with two faked photons. In this case the total transverse momentum of the charged particles $P_t^c = |\sum \mathbf{p}_t^c|$ is almost zero. To reduce this background a cut $P_t^c > 0.05$ GeV is applied.
– The second kind are events which contain a faked π^0 signal. Photon candidates might be noise signals.
– The third kind are events where one or more particles escape detection.

Events due to $\pi^+\pi^-\pi^0$ and to background have quite different total transverse momentum $P_t = |\sum \mathbf{p}_t|$ distribution. Figure 2 shows the fit of the experimental distribution with the Monte Carlo prediction for $\pi^+\pi^-\pi^0$ events and, in addition, the second-order polynomial. The side bands of the π^0 mass (65–95 MeV and 155–185 MeV) distribution is also shown. The two different background estimations agree that the background level is small. To reduce the background a cut $P_t < 0.10$ GeV is used. The background is a strong function of the $\pi^+\pi^-\pi^0$ mass ($W_{\gamma\gamma}$) (fig. 3): the background is high at small $W_{\gamma\gamma}$ and becomes smaller than 10% for $\pi^+\pi^-\pi^0$ masses higher than 1.2 GeV.

The $\pi^+\pi^-\pi^0$ mass distribution shown in fig. 4a is dominated by the production of $a_2(1320)$. In addition there is a shoulder in the 1.6–1.8 GeV mass region.

The main signal in the $\pi^\pm\pi^0$ mass spectrum, presented in fig. 4b, is due to $\rho(770)$. There is very little structure in the region above 1 GeV and almost no events above 1.5 GeV.

The $\pi^+\pi^-$ mass distribution is shown in fig. 4c. For a three-pion mass above 1.5 GeV, $f_2(1270)$ is present, as shown in fig. 4d.

In all mass distributions of fig. 4 the background, estimated from the side bands of π^0, is indicated as a shaded histogram.

The total selection efficiency rises from 0.3% at $W_{\gamma\gamma} = 1$ GeV to 4.5% at $W_{\gamma\gamma} = 5$ GeV. The acceptance of the detector and the efficiency of the analysis are calculated by Monte Carlo. The efficiencies of the first-level (charged particles) and higher-levels triggers depend on the year

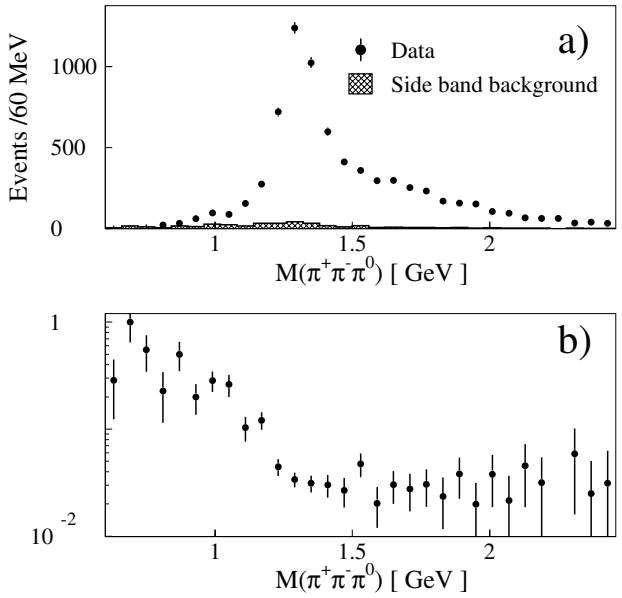

Fig. 3. a) Mass spectra $M(\pi^+\pi^-\pi^0)$ for the selected events. The background, estimated from the side bands of π^0, is shown as a shaded area. b) Ratio of the background contribution to the number of selected events.

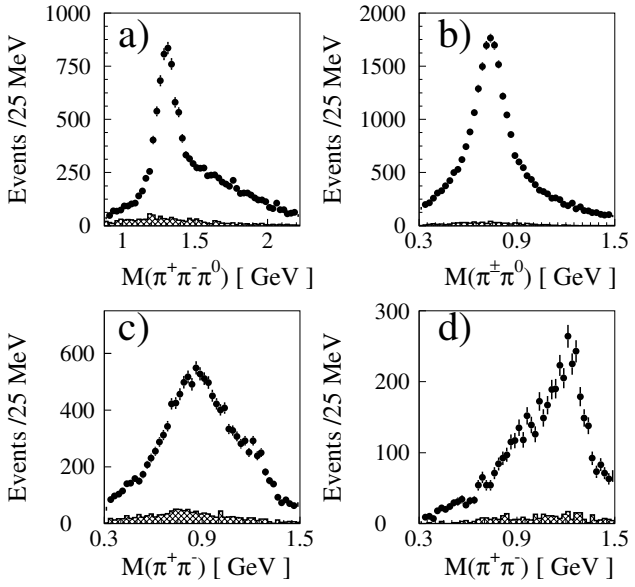

Fig. 4. Mass spectra for the selected events: a) $M(\pi^+\pi^-\pi^0)$; b) $M(\pi^\pm\pi^0)$ (two entries per event); c) $M(\pi^+\pi^-)$; d) $M(\pi^+\pi^-)$ with 3 pion mass higher than 1.5 GeV. The background, estimated from the side bands of π^0, is shown as a shaded area.

of data taking: they are calculated directly from the data and vary from $\sim 40\%$ at low $W_{\gamma\gamma}$ to $\sim 90\%$ at high $W_{\gamma\gamma}$.

3 Energy-dependent partial wave analysis

The measured cross-section $\mathrm{d}\sigma$ in the phase space $\mathrm{d}\Phi$ for the two-photon transition into three pions is written in the two-photon center-of-mass as

$$\frac{\mathrm{d}\sigma}{\mathrm{d}\Phi} = \frac{(2\pi)^4}{2W_{\gamma\gamma}^2}(|A|^2 + BG). \tag{1}$$

The background contribution BG is parameterized by a second-order polynomial, depending on an effective mass of 3 pions system $W_{\gamma\gamma}$.

The analysis is largely based on the method of extraction of leading singularities, suggested in [10]. The amplitude for the two-photon interaction is written as

$$A = \sum_i \epsilon_\mu^{(1)} \epsilon_\nu^{(2)} A_{\mu\nu}^i. \tag{2}$$

Here, ϵ_μ are the polarization vectors of the photons and the index i describes three possible spin configurations, 0, 1, or 2, of the two-photon system. Only scalar and tensor states are allowed for real photons. After averaging over the polarization of the initial photons, the amplitudes are orthogonal.

The amplitude $A_{\mu\nu}^i$ for the cascade from resonance R to R' via π emission $R \to R'\pi$ is expressed as the product of Breit-Wigner amplitudes and the angular momentum operator $O_{\mu\nu}^{\alpha,i,l,j,m}$:

$$\begin{aligned} A_{\mu\nu}^i = \sum_{\alpha,l,j,m} & \left(\frac{g_{il}^\alpha A_{jm}^\alpha}{M_\alpha^2 - W_{\gamma\gamma}^2 - iM_\alpha\Gamma_\alpha} \right) \\ & \times \frac{O_{\mu\nu}^{\alpha,i,l,j,m}}{\sqrt{F(q,r,l)F(k^\perp,r,m)F(k_{12},r,j)}} \\ & \times \frac{1}{M_j^2 - s_{12} - iM_j\Gamma_j}\,; \end{aligned} \tag{3}$$

$$\begin{aligned} P &= k_1 + k_2 + k_3, \\ k_\mu^\perp &= \frac{1}{2}\left(k_{1\mu} + k_{2\mu} - k_{3\mu} - \frac{s_{12} - m_\pi^2}{W_{\gamma\gamma}^2}\, P_\mu \right), \\ k_{12\mu} &= \frac{1}{2}(k_{1\mu} - k_{2\mu}), \qquad q = \frac{1}{2}W_{\gamma\gamma}, \qquad P^2 = W_{\gamma\gamma}^2, \\ s_{12} &= (k_1 + k_2)^2, \\ k^\perp &= \sqrt{-k_\mu^\perp k^{\perp\mu}}\,, \qquad k_{12} = \sqrt{-k_{12\mu}k_{12}^\mu}\,. \end{aligned}$$

Here the index α refer to the total spin of R, the indices i, l to the spin and orbital angular momentum of the $\gamma\gamma$ system and j, m to the spin of R' and its orbital angular momentum with the spectator pion. The functions F are Blatt-Weisskopf factors [11] for a system with interaction radius r. There is a weak dependence on this radius which in this analysis is fixed to 0.8 fm. The widths of R and R' resonances were parameterized as the sum of partial widths from well-known decay modes normalized to the total width of the state:

$$\Gamma = \frac{\Gamma_{tot}}{\sum \Gamma_i} \sum \Gamma_i \frac{k_i^{2L_i+1} F(k_{iM}, r, L_i)\; M}{k_{iM}^{2L_i+1} F(k_i, r, L_i)\; \sqrt{s}}\,. \tag{4}$$

Here k_i ($k_{iM} = k_i(s = M^2)$) is the relative momentum and L_i is the orbital momentum in the decay channel i. The ratio of partial widths are taken from PDG [12]. For example, the width of $a_2(1320)$ state was parameterized as sum of $\rho\pi$ and $\eta\pi$ partial widths with relative proportion in the resonance mass 0.71/0.15. The width of $a_2(1700)$ state where branching ratios are not very well known was parameterized with energy dependence from $\rho\pi$ phase space.

The operators $O_{\mu\nu}^{\alpha,i,l,j,m}$ describe the tensor structure of the $\gamma\gamma \to \pi^+\pi^-\pi^0$ amplitude; the explicit form of these operators can be found in [3].

The couplings of resonances with the $\gamma\gamma$ channel, g_{il}^{α}, are real numbers. Three-body decay couplings Λ_{jm}^{α}, which includes the two-body coupling for the decay of R' into two pions, are complex numbers. Masses and widths of R' resonances were fixed to PDG values [12].

4 Fit of the data

From the four-vectors of each event (j) a likelihood function is constructed as

$$L = \frac{1}{\sigma_{tot}} \prod_j \frac{\mathrm{d}\sigma_j}{\mathrm{d}\Phi} = \frac{1}{\sum\limits_n^{MC} \mathrm{d}\sigma_n} \prod_j \frac{\mathrm{d}\sigma_j}{\mathrm{d}\Phi}\,, \qquad (5)$$

where σ_{tot} is the integrated cross-section over the available phase space, calculated as the sum of all Monte Carlo events that passed the detector acceptance and the selection cuts. The parameters of the different states are the pole mass, the couplings and the widths of the resonances R as well as the parameters of the polynomial background.

In order to fit the data we consider the 2π resonance $\rho(770)$ and $f_2(1270)$ clearly observed in the $\pi\pi$ spectra. There is no need to introduce either $\rho_3(1690)$ or $\rho(1770)$, however a contribution of the broad state $\rho(1450)$ [12] is required to describe the data. There are no clear signals either from the narrow $f_0(980)$ or from $f_0(1500)$. Being included in the fit they give negligible contributions and therefore we omitted them in the final solution. The $\pi\pi \to \pi\pi$ S-wave amplitude is included, as a broad component which covers the mass region from the $\pi\pi$ threshold up to 2 GeV. It is parameterized in the framework of the P-vector/K-matrix approach [13]. All three solutions given in this article were tried in the fit. However due to limited phase space we did not find any notable difference from using any of the parameterizations. Moreover we could not really fix unambiguously the parameters of the P-vector. We obtained a very similar answer using either two production couplings of lowest K-matrix poles or one pole coupling and a nonresonant $\pi\pi$ production.

We have performed a number of fits with different combinations of resonances and background. To describe the two-pion masses and all angular distributions in the whole $W_{\gamma\gamma}$ interval we need three tensor states[1]: $a_2(1320)$, $a_2(1700)$ and $a_2(2030)$, a pseudoscalar meson which can be identified with $\pi(1300)$ and a 2^{-+} state at high mass. This hypothesis gives a good description of the $\pi^+\pi^-\pi^0$ mass spectrum, as shown in fig. 5. A χ^2 comparison gives a confidence level of 30%. The $\pi\pi$ mass distributions, the angular distributions of pions in $\gamma\gamma$ center of mass and the angular distributions between one pion from the $\pi\pi$ system and a spectator pion (in respect to this system) calculated in the system center of mass are shown in fig. 6 and fig. 7 for the regions of the most prominent states, $a_2(1320)$ and $a_2(1700)$. A χ^2 comparison for these plots gives confidence levels in the range of 20 to 40%. If we exclude some of the states, we fail to describe the angular distributions and the branching ratios of $a_2(1320)$ to $f_2(1270)\pi$ and $\rho(1450)\pi$ (which can be calculated in respect to the $\rho(770)\pi$ branching ratio) get unreasonably high values. To study the stability of the final solution (see table 1) we add one by one resonances with different quantum numbers, but no other state gives a significant contribution.

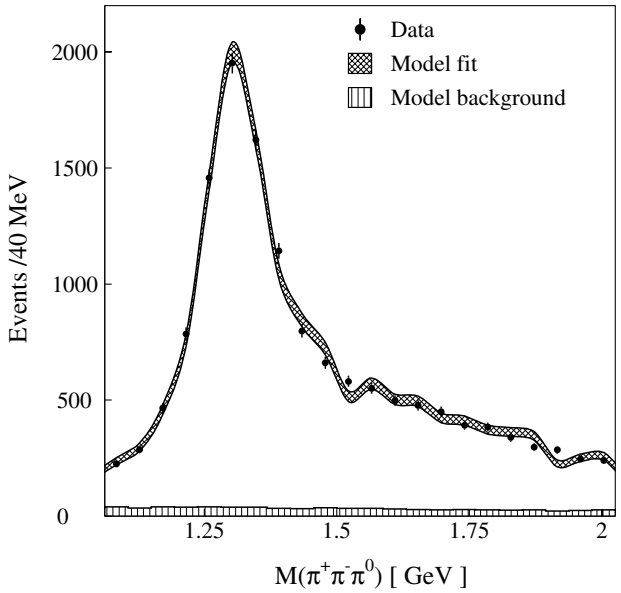

Fig. 5. The $\pi^+\pi^-\pi^0$ mass distribution of the data (full points) compared to the one obtained by the partial wave analysis fit (fit curve with corridor of statistical errors including MC limited statistics).

The oscillatory behavior of the description curves in figs. 6 and 7 is due to the limited number of the available Monte Carlo events. Remember that in the likelihood function the Monte Carlo events are only used for the normalization integral and local oscillations hardly can influence the solution. To check the stability of the solution we performed set of fits with smaller sample and with Monte Carlo events selected with larger P_t.

The statistical errors are calculated by the minimization program. Systematic uncertainties on the masses, widths and couplings are evaluated taking into account:

– Cut variation. The fit is repeated with a $P_t \leq 0.05$ GeV cut to investigate a possible P_t-dependence.

[1] The names of the resonances are taken from PDG [12].

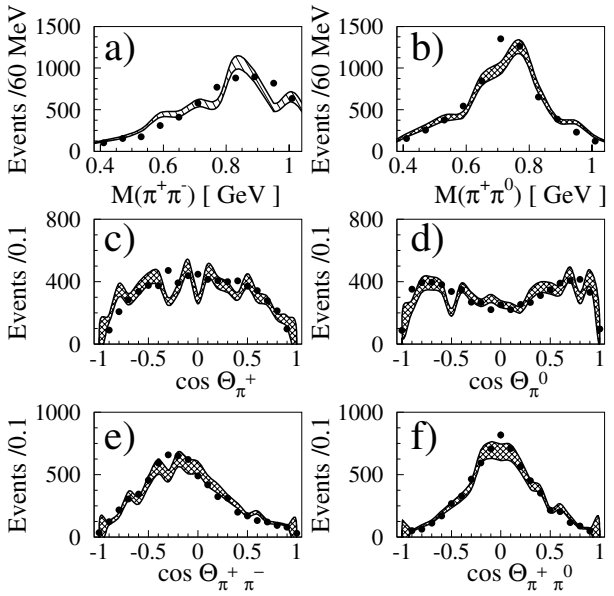

Fig. 6. The distributions of the mass and angular variables for data (full points) and partial wave analysis (curve with shaded corridor of statistical errors) for the mass interval $1200 \leq W_{\gamma\gamma} \leq 1400\,\mathrm{MeV}$. a) The $\pi^+\pi^-$ mass; b) the $\pi^0\pi^\pm$ mass; c) the angle of the charged pion in the center of mass of the reaction; d) the angle of the neutral pion in the center of mass of the reaction; e) the angle between positive and negative pions in the $\pi^+\pi^0$ center of mass; f) the angle between neutral and negative pions in $\pi^+\pi^-$ center of mass.

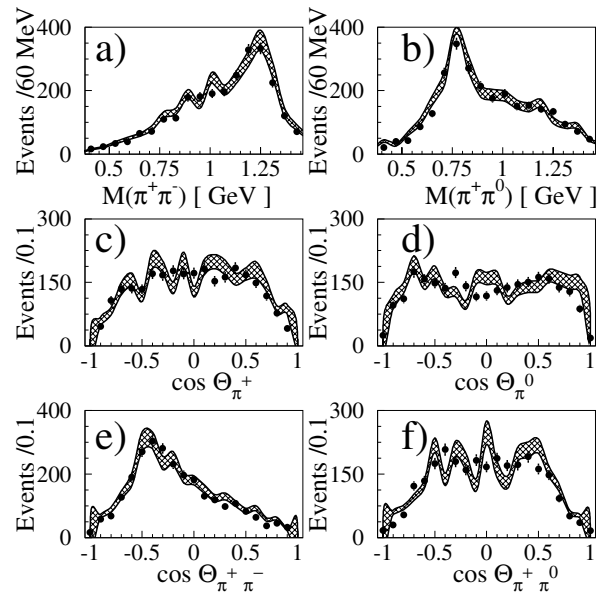

Fig. 7. The distributions of the mass and angular variables for data (full points) and partial wave analysis (curve with shaded corridor of statistical errors) for the mass interval $1600 \leq W_{\gamma\gamma} \leq 1900\,\mathrm{MeV}$. a) The $\pi^+\pi^-$ mass; b) the $\pi^0\pi^\pm$ mass; c) the angle of the charged pion in the center of mass of the reaction; d) the angle of the neutral pion in the center of mass of the reaction; e) the angle between positive and negative pions in the $\pi^+\pi^0$ center of mass; f) the angle between neutral and negative pions in $\pi^+\pi^-$ center of mass.

Table 1. Masses and widths of resonances included into the fit. The name of the resonances is taken from ref. [12].

Resonance	M, GeV	Γ, GeV
$\rho(770)$	0.776	0.149
$\rho(1450)$	1.465	0.310
$f_2(1270)$	1.275	0.185
$S(\pi\pi)$	K-matrix	[13]
$a_2(1320)$	free	free
$a_2(1700)$	free	free
$a_2(2030)$	free	free
$\pi(1300)$	free	free
2^{-+}	free	free
$\pi_2(1670)$	1670	260

– Uncertainties due to different running conditions. The solution is checked by fitting every year data sample separately.
– Change the number of resonances R, in particular fits which takes into account only a_2 resonances.

5 Discussion

The individual contributions to the cross-section $\gamma\gamma \to \pi^+\pi^-\pi^0$, proportional to $|A^i_{\mu\nu}|^2$, are shown in fig. 8. It is seen that the sum of individual cross-sections differs from the total cross-section due to interference between overlapping 2^{++} states. The resonance masses obtained from the fit are corrected because of an instrumental effect found from MC simulation. Masses are decreased by 1 MeV for $a_2(1320)$ and by 6 MeV for $a_2(2030)$. Corrections have

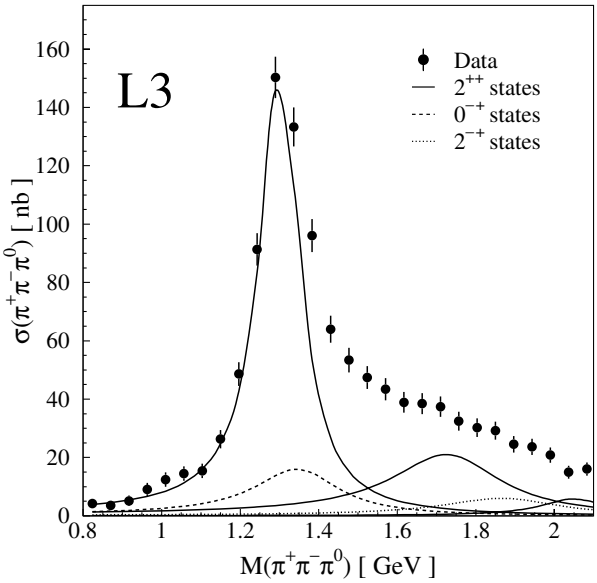

Fig. 8. The contribution of the resonances to the cross-section. The full cross-section of $\gamma\gamma \to \pi^+\pi^-\pi^0$ reaction is calculated for $P_t < 0.1\,\mathrm{GeV}$ cut and shown as points with error bars. Three full curves correspond to three 2^{++} states, the dashed curve to the 0^{-+} and the dotted curve to the 2^{-+} contributions.

Table 2. Masses, widths and the products of $\Gamma_{\gamma\gamma}\ Br(3\pi)$ for the observed resonances. The name of the resonances is taken from ref. [12].

Resonance	M, MeV	Γ, MeV	$\Gamma_{\gamma\gamma}Br(3\pi)$, keV	Fitted decay modes
$a_2(1320)$	$1300 \pm 2 \pm 4$	$117 \pm 6 \pm 20$	$0.65 \pm 0.02 \pm 0.02$	$\rho(770)\pi$, $\rho(1450)\pi$, $f_2\pi$
$a_2(1700)$	$1722 \pm 9 \pm 15$	$336 \pm 20 \pm 20$	$0.37^{+0.12}_{-0.08} \pm 0.10$	$\rho(770)\pi$, $\rho(1450)\pi$, $f_2\pi$
$a_2(2030)$	$2050 \pm 10 \pm 40$	$190 \pm 22 \pm 100$	$0.11 \pm 0.04 \pm 0.05$	$\rho(770)\pi$
$\pi(1300)$	$1345 \pm 8 \pm 10$	$260 \pm 20 \pm 30$	$\leq 0.8(.95CL)$	$\rho(770)\pi$, $S(\pi\pi)\pi$, $f_2\pi$
2^{-+}	$1860 \pm 12 \pm 10$	$352 \pm 30 \pm 40$	$0.15 \pm 0.03 \pm 0.05$	$\rho(770)\pi$, $f_2\pi$
$\pi_2(1670)^*$	1670	260	$\leq 0.1(.95CL)$	$\rho(770)\pi$, $f_2\pi$

* The 2^{-+} signal is fixed as $\pi_2(1670)$ with values taken from ref. [12].

been applied for the width measurements to take into account the experimental resolution of 50–60 MeV.

5.1 $a_2(1320)$

The mass and width of $a_2(1320)$, obtained by the fit, are listed in table 2. The measured mass $1.300 \pm 0.002 \pm 0.004$ GeV is 18 MeV lower than the world average [12], since in our fit the mass is the pole of the amplitude and not the central value of the mass spectrum. The central value of the mass spectrum depends also on the way of taking into account a contribution of wide resonances ($a_2(1700)$ and $\pi(1300)$). A fit using Breit-Wigner amplitudes with a mass-dependent width was performed with an event selection similar to an earlier L3 publication [2]. The fit gives the mass $1.326 \pm 0.002 \pm 0.010$ GeV, but this value depends on the selection cuts and the background parameterization.

The $a_2(1320)$ is produced dominantly from the ${}^5S_2$ (the notation ${}^{2s+1}L_J$ is used here to describe the two-photon initial state) state. The ratio for the production from ${}^5S_2$ and ${}^1D_2$ is found to be

$$\frac{\sigma(\gamma\gamma({}^5S_2) \to a_2(1320))}{\sigma(\gamma\gamma({}^1D_2) \to a_2(1320))} = 8.2 \pm 0.6 \pm 0.1. \qquad (6)$$

According to the definitions of ref. [3], this corresponds[2] to a ratio for the couplings g_{ik} of 1.30 ± 0.25. This value is in agreement with the theoretical expectation [14] of 0.95 ± 0.15, for an interaction radius of 0.6–0.8 fm.

The contribution of this resonance to the cross-section is very stable in all fits, $\Gamma_{\gamma\gamma}$ is therefore well measured. The value obtained for the product of $\Gamma_{\gamma\gamma}$ with the 3π branching ratio, $Br(3\pi)$, is given in table 2 with statistical and systematic uncertainties.

The fitted decay modes of $a_2(1320)$ are listed in table 2. The resonance dominantly decays into $\rho(770)\pi$ in agreement with earlier analyses (see [12]). However, we found that introduction of the $f_2(1270)\pi$ and $\rho(1440)\pi$ decay channels improves the quality of the fit. The contribution of these channels were found to be on the level of 5% from the $\rho(770)\pi$ mode and heavily correlated with the $a_2(1700)$ decay modes.

[2] This calculation involves extracting Blatt-Weisskopf barrier factors which were not introduced in [3].

5.2 $a_2(1700)$ resonance

This state was observed in the first analysis of the L3 data [2] with limited statistics. The mass was found to be $1752 \pm 21 \pm 4$ MeV and the width $150 \pm 110 \pm 34$ MeV. This state is confirmed by the present full statistics analysis. Its contribution depends on the interference of this state with the tail of $a_2(1320)$. Mass, width and two-photon width obtained here are listed in table 2 as well as fitted decay modes. These values are compatible with the previous observation. Taking into account errors indicated by the Crystal Barrel collaboration for $a_2(1700)$ [15], it is possible that the same state is observed in both experiments.

The fitted decay modes of $a_2(1700)$ are listed in the table 2. The resonance has a significant branching ratio into $f_2(1270)\pi$:

$$\frac{Br(a_2(1700) \to \rho(770)\pi)}{Br(a_2(1700) \to f_2(1270)\pi)} = 3.4 \pm 0.4 \pm 0.1. \qquad (7)$$

This contribution is well seen on the mass slice in the resonance mass region (see fig. 7a). The fit also indicated a possible contribution from $\rho(1450)\pi$ but it was found much less stable due to correlation with other decay modes and the tail from the $a_2(1320)$ state.

The ratio for the production of the resonance from ${}^5S_2$ and from ${}^1D_2$ two-photon initial states is found to be

$$\frac{\sigma(\gamma\gamma({}^5S_2) \to a_2(1700))}{\sigma(\gamma\gamma({}^1D_2) \to a_2(1700))} = 2.5 \pm 1.0 \pm 0.1. \qquad (8)$$

The corresponding coupling ratio is 0.60 ± 0.20, well in agreement with the expectation [14] for the first tensor radial excitation 0.54 ± 0.16.

These results can be compared with the calculations of the relativistic quark models for meson radial excitations ([16] and references therein). The fitted mass is consistent with the One Gluon Exchange Semi-Relativistic Quark Mass model [16] which predicts a mass of 1740 MeV.

5.3 $a_2(2030)$ resonance

At higher $W_{\gamma\gamma}$ we need a contribution from another isovector tensor state. Only the $\rho(770)\pi$ decay mode is taken into account. The contribution of this resonance to the cross-section is found to be stable and the product of $\Gamma_{\gamma\gamma}$ and $Br(3\pi)$, given in table 2, can be reliably calculated.

5.4 0^{-+} states and the experimental background

The likelihood value is significantly improved if the $\pi(1300)$ state is introduced in the analysis. Its contribution to the cross-section is the third largest one after $a_2(1320)$ and $a_2(1700)$. However, the ratio between the $\pi(1300)$ and $a_2(1320)$ contributions has some P_t-dependence which can be interpreted as an influence of a background. A 0^{-+} state is produced from the $^1S_0$ $\gamma\gamma$ partial wave and therefore in nonpolarized experiment can only interfere with the $^1D_2$ tensor partial wave. The last was found to be much smaller then the $^5S_2$ amplitude and therefore the pseudoscalar state weakly interferes with the tensor states in the reaction investigated. Moreover, a 0^{-+} state produces a uniform angular distribution in $\gamma\gamma \to \pi^+\pi^-\pi^0$ similar to a noncoherent background contribution. Considering that the signal-to-noise ratio is very low in the mass region below 1.2 GeV, as shown in fig. 1a, we can only estimate an upper limit for the $\gamma\gamma$ width of this state. It is listed in table 2 together with the fitted values of mass and width.

5.5 π_2 signal

A 2^{-+} signal is found in the mass region 1850–1900 MeV. It can be partly related to $\pi_2(1670)$ [12]. However, fixing the 2^{-+} signal to the parameters of $\pi_2(1670)$ makes the likelihood worse and if the mass is left free it always moves to the 1850–1900 MeV region and the signal becomes stronger. Therefore from the present analysis we can only give an upper limit for the $\gamma\gamma$ width of $\pi_2(1670)$ and to point out a possible presence of a 2^{-+} signal in 1850–1900 MeV mass region. These values are given in table 2.

5.6 Tensor meson masses with reduced parameters set

A special fit is done with only isovector tensor mesons to check the stability of resonance parameters. In this case we find:

$a_2(1320)$ mass: 1303 ± 2 MeV; width: 140 ± 4 MeV;
$a_2(1700)$ mass: 1709 ± 9 MeV; width: 340 ± 20 MeV;
$a_2(2030)$ mass: 2014 ± 14 MeV; width: 350 ± 32 MeV.

These changes are included in the systematic errors.

6 Conclusion

The high statistics sample of $e^+e^- \to e^+e^-\pi^+\pi^-\pi^0$ events collected by L3 at LEP allows an accurate amplitude analysis of the three-pion final state. In addition to the dominant $a_2(1320)$ we have to include two more isovector tensor states, $a_2(1700)$ and $a_2(2030)$. They can be interpreted as $a_2(1320)$ radial excitations. The presence of the 0^{-+} and 2^{-+} waves is also necessary to describe the data.

We are very grateful to V.V. Anisovich for extremely useful discussions and comments. V.A. Schegelsky thanks the members of L3 Collaboration, especially S.C.C. Ting, for constructive discussions. This work was partly supported by the Russian Foundation for Basic Research (grant 04-02-17091).

References

1. JADE Collaboration (J.E. Olsson), *Proceedings of the V International Conference on Two-Photon Physics, Aachen, 1983*, edited by Ch. Berger (Springer, Berlin, 1983); CELLO Collaboration (H.J. Behrend *et al.*), Phys. Lett. B **114**, 378 (1982); Phys. Lett. **125**, 518 (1983); Z. Phys. C **46**, 583 (1990); Pluto Collaboration (Ch. Berger *et al.*), Phys. Lett. B **149**, 427 (1984); TASSO Collaboration (M. Althoff *et al.*), Z. Phys. C **31**, 537 (1986); MARK2 Collaboration (F. Butler *et al.*), Phys. Rev. D **42**, 1368 (1990); MD1 Collaboration (S.E. Baru *et al.*), Z. Phys. C **48**, 581 (1990); ARGUS Collaboration (E. Kriznic), Nuovo Cimento A **107**, 11 (1994); ARGUS Collaboration (H. Albrecht *et al.*), Z. Phys. C **74**, 469 (1997).
2. L3 Collaboration (M. Acciari *et al.*), Phys. Lett. B **413**, 147 (1997).
3. A.V. Anisovich *et al.*, J. Phys. G **28**, 15 (2002).
4. F. Linde, *Workshop on Detector and Event Simulation in High Energy Physics Monte Carlo, Amsterdam, 1991*, edited by K. Bos, B. van Eijl (NIKHEF, Amsterdam, 1991).
5. R. Brun *et al.*, GEANT 3.15 preprint CERN DD/EE/84-1 (revised 1987).
6. H. Fesefeldt, RWTH Aachen report PITHA 85/2 (1985).
7. L3 Collaboration (B. Adeva *et al.*), Nucl. Instrum. Methods A **289**, 35 (1990); M. Acciarri *et al.*, Nucl. Instrum. Methods A **351**, 300 (1994); M. Chemarin *et al.*, Nucl. Instrum. Methods A **349**, 345 (1994); A. Adam *et al.*, Nucl. Instrum. Methods A **383**, 342 (1996).
8. P. Béné *et al.*, Nucl. Instrum. Methods A **306**, 150 (1991).
9. D. Haas *et al.*, Nucl. Instrum. Methods A **420**, 101 (1999).
10. V.V. Anisovich *et al.*, Phys. At. Nucl. **57**, 1595 (1994).
11. F. Von Hippel, C. Quigg, Phys. Rev. D **5**, 624 (1972).
12. Particle Data Group (K. Hagiwara *et al.*), Phys. Rev. D **66**, 1 (2002).
13. V.V. Anisovich, Yu.D. Prokoshkin, A.V. Sarantsev, Phys. Lett. B **389**, 388 (1996).
14. A.V. Anisovich, V.V. Anisovich, V.A. Nikonov, Eur. Phys. J. A **12**, 103 (2001).
15. Crystal Barrel Collaboration (C. Amsler *et al.*), Phys. Lett. B **333**, 277 (1994); Eur. Phys. J. C **23**, 29 (2002).
16. C.R. Münz, Nucl. Phys. A **609**, 364 (1996).